Combustion Science and Technology

Decomposition and Ignition Characteristics of Titanium Hydride at High Heating Rates

Gregory Young[a], Guoqiang Jian[b], Rohit Jacob[b] & Michael R. Zachariah[b]

[a] Naval Surface Warfare Center-Indian Head Division, RDT&E Department, Indian Head, Maryland, USA

[b] University of Maryland, College Park, Maryland, USA
Accepted author version posted online: 02 Mar 2015.

CrossMark

Click for updates

PLEASE SCROLL DOWN FOR ARTICLE

Taylor & Francis
Taylor & Francis Group

DECOMPOSITION AND IGNITION CHARACTERISTICS OF TITANIUM HYDRIDE AT HIGH HEATING RATES

Gregory Young,[1] **Guoqiang Jian,**[2] **Rohit Jacob,**[2] **and Michael R. Zachariah**[2]

[1]*Naval Surface Warfare Center–Indian Head Division, RDT&E Department, Indian Head, Maryland, USA*
[2]*University of Maryland, College Park, Maryland, USA*

An experimental study was conducted to evaluate the decomposition, ignition, and combustion behavior of titanium hydride under high heating rate conditions. Samples were deposited on filaments, which were rapidly heated by joule heating under various conditions. Dehydrogenation experiments were conducted under vacuum conditions at heating rates of up to 4×10^5 K/s. The results of these experiments suggest that, at high heating rates, the onset of dehydrogenation is limited by intraparticle diffusion. The ignition and combustion behavior was studied in air and for ambient pressures ranging from atmospheric up to 7 MPa in a windowed pressure vessel. Broadband light emission was used to quantify the ignition temperature. The experiments revealed that the ignition temperature decreased linearly with increasing pressure from approximately 1700 K to 1475 K. Comparison of the dehydrogenation temperatures to the ignition temperatures over the entire pressure range suggests that the onset of the dehydrogenation process is not likely to be affected by ambient pressure. Finally, observation of the steady state combustion process by high speed imaging and post mortem analysis revealed many similar combustion characteristics to pure titanium. Particle explosions were observed and quenched particles were found to consist of titanium, nitrogen, and oxygen.

INTRODUCTION

Metal hydrides have received considerable attention as potential hydrogen storage media (Ahluwalia et al., 2009; Liu et al., 2009; Sakintuna et al., 2007; Samal et al., 2012; Stepura et al., 2012) and as fuel supplements in propellants (Connell et al., 2011; Shark et al., 2013; Young et al., 2010a). In fact, some metal hydrides even offer greater hydrogen storage density than liquid hydrogen (Sakintuna et al., 2007), making them a potentially more practical and safer alternative for the automobile industry. Titanium hydride has also found applications as a foaming agent for aluminum foam manufacturing processes and as a bonding material for glass or ceramics with metals (Kennedy, 2002; Kennedy and Lopez, 2003; Matijasevic-Lux et al., 2006; Samal et al., 2012).

The decomposition process of titanium hydride has been studied extensively by typical thermal analyses, such as thermal gravimetric analysis (TGA), differential scanning calorimetry (DSC), thermal desorption spectroscopy, and differential thermal analysis (DTA) (Borchers et al., 2009; Illekova et al., 2011; Liu et al., 2009; Rasooli et al., 2013; Samal et al., 2012; Stepura et al., 2012). Dehydrogenation typically starts at about 500°C (773 K) (Samal et al., 2012; Stepura et al., 2012), but has been reported as low as 390°C (663 K) (Matijasevic-Lux et al., 2006). Discrepancies on the onset of hydrogen release between researchers have been largely attributed to differences in sources for the materials as well as heating rates. The dehydrogenation process is endothermic, and is generally represented by a multistep process (Borchers et al., 2009; Illekova et al., 2011; Liu et al., 2009; Samal et al., 2012). Matijasevic-Lux et al. (2006) and Kennedy and Lopez (2003) showed that in an inert environment (argon), approximately 25 wt% of the hydrogen in TiH_2 is released during the first stage of decomposition to produce δ-$TiH_{1.5}$. Upon further heating, this sub-stoichiometric hydride further transforms to the β- and α-phases with further loss of hydrogen during the second stage of decomposition (Kennedy and Lopez, 2003).

Heating of titanium hydride in air results in a far different decomposition process. Exothermic events are observed in air that are near coincident with the endothermic events when heating in argon (Kennedy and Lopez, 2003). Following the exothermic events, further heating in air produces an endothermic event, which has been interpreted as further hydrogen release (Kennedy and Lopez, 2003). Both Gromov et al. (1997) and Kennedy and Lopez (2003) found evidence of oxyhydride and oxide formation while heating TiH_2 in air. According to Illekova et al. (2011), in the presence of oxygen, the dehydrogenation and oxidation processes are not competitive, but rather consecutive reactions. Illekova et al. (2011) suggests that the presence of oxygen gradually transforms the tetragonal TiH_2 lattice into the tetragonal TiO_2 (rutile) via formation of pure Ti and Ti_6O. Subsequently, the newly formed Ti-O surface layer slows down the further release of hydrogen from the bulk.

Although a great deal of work has been conducted on the decomposition of titanium hydride, relatively few works have been reported on its ignition and combustion behavior. Anderson and Fleshman (1950), using pressed pellets of titanium hydride, identified a critical ignition temperature of 885 K in static (open tube furnace) and dynamic (air flowing over sample) conditions. Hartmann (1951) found that dust clouds of titanium hydride particles ignite in air at 713 K.

While ignition and combustion data is scarce for titanium hydride, more information has been reported on the combustion behavior of pure titanium particles (Badiola and Dreizin, 2013; Clark et al., 1975; Harrison, 1958; Molodetsky et al., 1998; Shafirovich et al., 2008). In early studies, Harrison (1958) observed that titanium combustion takes place at the surface, without substantial vaporization of the metal. Clark et al. (1975) describes a three-stage combustion process for titanium in oxygen. The first stage includes heating and ignition, the second stage was described by a rapid drop in luminosity followed by steady burning with increasing intensity, and the third stage was characterized by the ejection of one or more particles from the specimen with decreasing luminosity. In addition, Clark et al. (1975) described frequent particle explosions or fragmentations. Molodetsky et al. (1998) confirmed the phenomenon of particle explosion while also measuring particle temperature history during combustion in air. The highest temperature measured was 2400°C, which is well below the boiling temperature of either titanium or its oxides further demonstrating that combustion takes place on the surface of the particle. In addition, Moledetsky et al. (1998) attributed the particle explosion phenomenon to the solubility of both oxygen and nitrogen in titanium. As the titanium particles move toward their final

oxide products, nitrogen gas is released exerting pressure on the burning particle leading to fragmentation.

In previous studies (Young et al., 2010b, in press), we found that the ignition temperature of aluminum hydride was a function of heating rate as well as pressure up until a critical pressure was reached (0.4 MPa). Furthermore, we found that at heating rates relevant to propellant combustion, the rate controlling process for dehydrogenation was an intraparticle diffusion limit. In this study we examine the basic decomposition, ignition, and combustion characteristics of titanium hydride under high heating rate conditions and elevated pressures analogous to our previous studies on aluminum hydride (Young et al., 2010b, in press).

METHOD OF APPROACH

The titanium hydride used in this study was purchased from Alfa Aesar and characterized as 99% pure and 1–3 μm in size from the supplier. Figure 1 is a scanning electron microscope (SEM) image of the titanium hydride particles, which shows them to be irregular in shape, with some particles considerably larger than 3 μm. In each of the subsequently described experiments, the titanium hydride was dispersed in hexane from which the samples were drawn into a syringe, deposited on a platinum filament with a diameter of approximately 75 μm, and given sufficient time to dry in ambient air prior to experiments.

Powder X-ray diffraction (XRD) was conducted on the as-received material to ensure the quality of the titanium hydride. The instrument used was a Bruker D8 Advance using CuKα radiation. Figure 2 provides the results obtained for the as-received titanium hydride, which indicate that the initial powder was identified as TiH$_2$ (JCPDS No: 65-4798) with a face-center cubic crystal structure.

Heated Filament Experiments

Similar to our previous work (Young et al., 2010b), we studied the dehydrogenation process of titanium hydride at heating rates up to $\sim 4 \times 10^5$ K/s by a custom designed temperature jump (T-Jump) coupled with a time-of-flight spectrometer under vacuum conditions. The system employed in this study utilized an in-house power supply capable of delivering heating rates of $\sim 6 \times 10^5$ K/s. For all of the experiments in this study, the T-jump system consisted of an ~ 76 μm diameter platinum wire, which was joule heated.
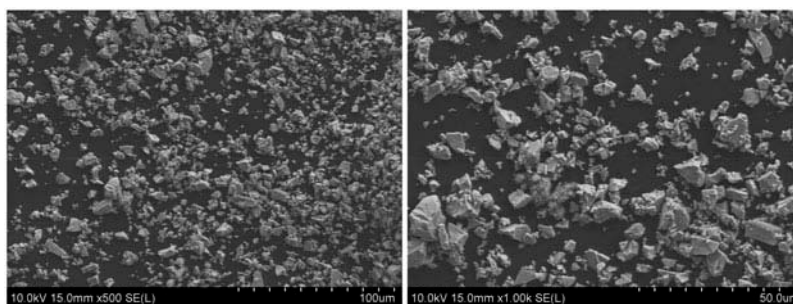

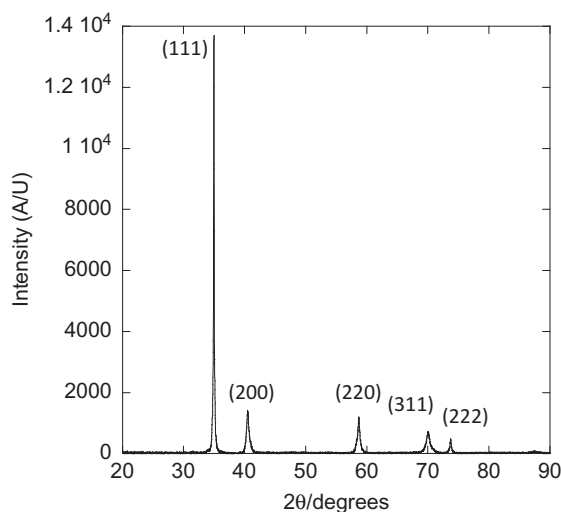**Figure 1** Scanning electron microscope images of titanium hydride particles.

Figure 2 XRD of as received TiH$_2$.

During the dehydrogenation experiments, heating rates ranging from approximately 8×10^4 K/s to 4×10^5 K/s were considered.

The ignition behavior of titanium hydride was also studied with the T-jump apparatus for pressures ranging from atmospheric up to about 7 MPa at an approximately constant heating rate of 1.3×10^5 K/s. Heating filaments coated with samples were inserted into a 0.1 liter pressure vessel rated to 24.1 MPa. The pressure vessel had three quartz windows providing optical access. Two windows were located at the same vertical height as the heating filament, and a third window was located at the bottom of the pressure vessel looking upward at the sample. The T-jump pressure vessel assembly can be seen schematically in Figure 3. Pressure was monitored and recorded with a Setra Model 206 static pressure transducer. A K-type thermocouple was also installed in the pressure vessel to ensure that samples would not be significantly heated by adiabatic compression during the pressurization process. The highest temperature rise associated with the pressurization process was about 5 K.
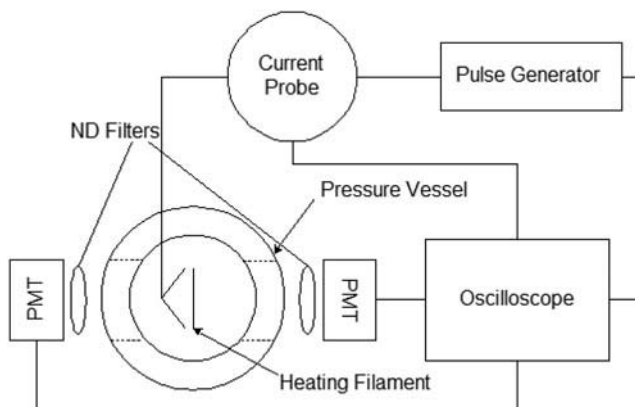

Figure 3 Schematic diagram of high pressure T-jump set up.

All ignition experiments were conducted with air as the oxidizing/pressurizing gas. Two Hamamatsu model H7827-012 photomultiplier tubes (PMTs), with a spectral range of 300–850 nm, were used to monitor broadband light emission in real-time to characterize ignition, with the output sent directly to an oscilloscope. Ignition was defined as 2% maximum light intensity collected by the PMTs as in our previous studies (Young et al., 2010b, in press). In addition, high speed imaging with and without backlighting was employed to provide further details on the ignition and combustion process of titanium hydride. During some experiments, a SEM stage was placed in close proximity (∼2.5 mm) to the heating filament to catch and quench burning particles for post mortem inspection. The temperature of the heating filament was deduced from a blackbody calibration with a resistance calculated from the voltage and current record (Jian et al., 2013).

RESULTS AND DISCUSSION

Decomposition Characteristics

The onset of dehydrogenation of the titanium hydride was determined in a similar fashion as we had previously done for aluminum hydride (Young et al., 2010b). The results can be seen in Figure 4. At our lowest heating rate (∼8×10^4 K/s) dehydrogenation begins at approximately 870 K and gradually increases to almost 1000 K at our highest heating rate (4×10^5 K/s). The observed increase in dehydrogenation temperature with heating rate is approximately linear and consistent with our aluminum hydride observations (Young et al., 2010b). At our lowest heating rate the dehydrogenation temperature of 870 K is approximately 100 K higher than that reported by other researchers (Liu et al., 2009; Samal et al., 2012; Stepura et al., 2012), but expected considering the heating rates used in this study are several orders of magnitude higher.
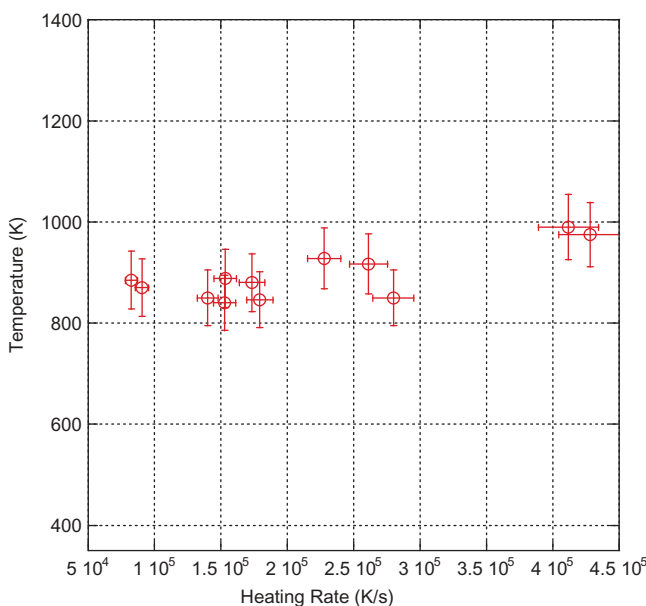

Figure 4 Hydrogen release temperature of TiH$_2$ for heating rates ranging from ∼8×10^4 K/s to ∼4.5×10^5 K/s.
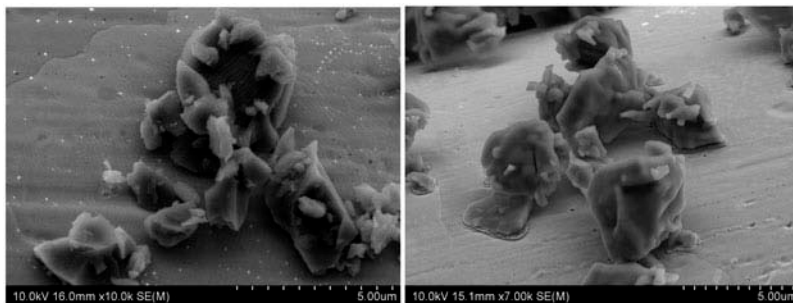
Figure 5 SEM images of titanium hydride to various temperatures under vacuum conditions (left: 970 K, right: 1110 K).

We also conducted a series of experiments with titanium hydride in which we heated the samples to a specified temperature under vacuum so that we could conduct a post-mortem analysis by SEM, which can be seen in Figure 5. When heated to 970 K, which is well into the dehydrogenation regime, we observe some particle deformation, which further increases and shows some melting at 1100 K, as should be expected since the melting temperature of TiH_2 is about 723 K. Samal et al. (2012) presented images of TiH_2 after heating to 1200 K in an oxidizing environment, which shows a continuous protective film on the surface, but the particles do not appear to have experienced any considerable melting. This suggests that the partial oxidation, which can occur during the dehydrogenation process of the particle, prevents it from melting, whereas in our experiments under vacuum, no oxidation took place allowing the particle to melt. Kennedy and Lopez (2003) suggests that in air the formation of oxyhydrides coincides with the onset temperature of hydrogen release in argon, while Fokin et al., (1995) suggests that oxygen implantation into the TiH_2 structure can occur without hydrogen loss, as oxygen can fill the existing octahedral vacancies. Whether oxyhydrides or oxides are formed, the melting temperature of the material can be greatly altered explaining the differences in observations between our work and Samal et al.'s (2012) work.

Plotting the reciprocal of the dehydrogenation temperature along with the natural logarithm of the heating rate in Figure 6 allows us to extract the activation energy associated with the onset of dehydrogenation by the Ozawa method (Ozawa, 1965, 1970). We find that the activation energy for the onset of dehydrogenation is about 47 kJ/mol, which is between 1/3 and 1/4 of the value provided by other researchers (Illekova et al., 2011; Liu et al., 2009) for the initial dehydrogenation step at lower heating rates. This is consistent with our observation with aluminum hydride (Young et al., 2010b) and is an indication of a change in decomposition mechanism to one that is limited by intraparticle diffusion, since this activation energy is too low to be representative of bond breaking. It should be pointed out that this activation energy was determined in vacuum, and is only intended to identify the onset of dehydrogenation. In oxygenated environments the overall dehydrogenation process is likely to be complicated by the formation of oxides and oxyhydrides.

Determination of Ignition Temperature

Ignition temperature was determined using the broadband light emission signal from two PMTs using 2% maximum light intensity as the definition of ignition as in our
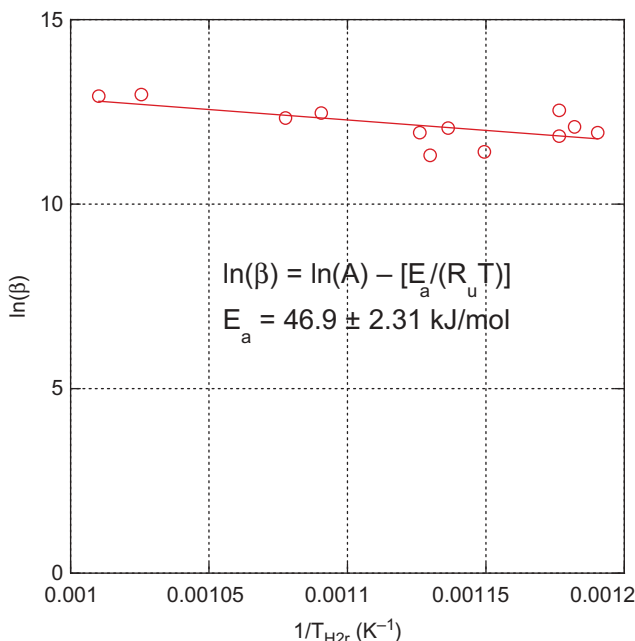
Figure 6 Arrhenius plot of TiH$_2$ decomposition for heating rates ranging from $\sim 8 \times 10^4$ K/s to $\sim 4.5 \times 10^5$ K/s based on the Ozawa method.

previous studies (Young et al., 2010a, in press). A background signal was taken for each experiment and subtracted off of the raw signal in the determination of ignition temperature. Figure 7 provides representative PMT signals for atmospheric pressure (0.101 MPa) conditions and for elevated pressure conditions (3.5 MPa and 7 MPa). From the figure it is clear that the ignition event is occurring sooner as the pressure is increased suggesting that the ignition temperature decreases as the pressure increases. Interestingly, at all three conditions shown, there appears to be two main regimes of burning based on the emission signals. In each case there is a rapid high intensity event followed by a lower intensity longer duration event. Similar light emission behavior was observed with titanium particle combustion in air by both Shafirovich et al. (2008) and Badiola and Dreizin (2013). At 7 MPa, the emission signal becomes even more interesting as the initial high intensity event is followed by a longer duration, lower intensity, and what appears to be a relatively high frequency, high amplitude event in comparison with the lower pressure examples. This was a consistent phenomenon only observed at our highest pressures.

Titanium hydride exhibits an approximately linear decrease in ignition temperature over the pressures ranging from atmospheric to about 5.3 MPa, after which there is a sharper decrease in the measured ignition temperature up to 7 MPa (Figure 8). The data shown in Figure 8 represent an average ignition temperature taken over 3 to 4 experiments per condition. At atmospheric pressure, the ignition temperature was about 1700 K and dropped to about 1475 K as the pressure was increased to 7 MPa. These ignition temperatures are significantly higher than those reported by Anderson and Fleshman (1950) and Hartman
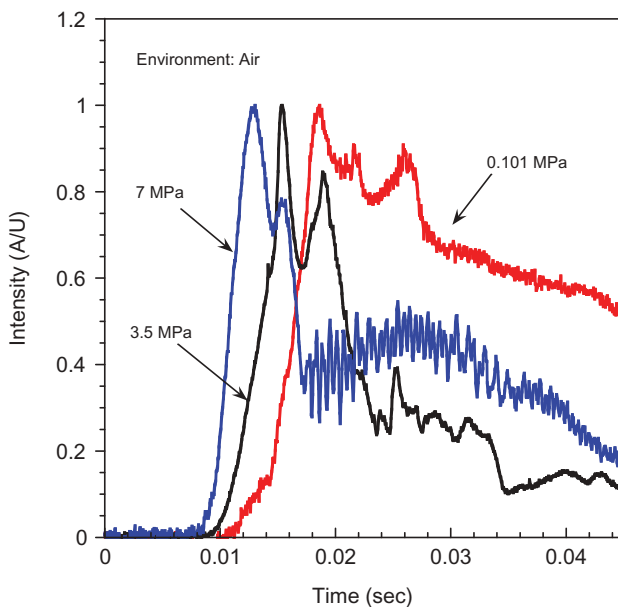
Figure 7 PMT traces of titanium hydride/air ignition at pressures of 0.101 MPa and 3.5 MPa.
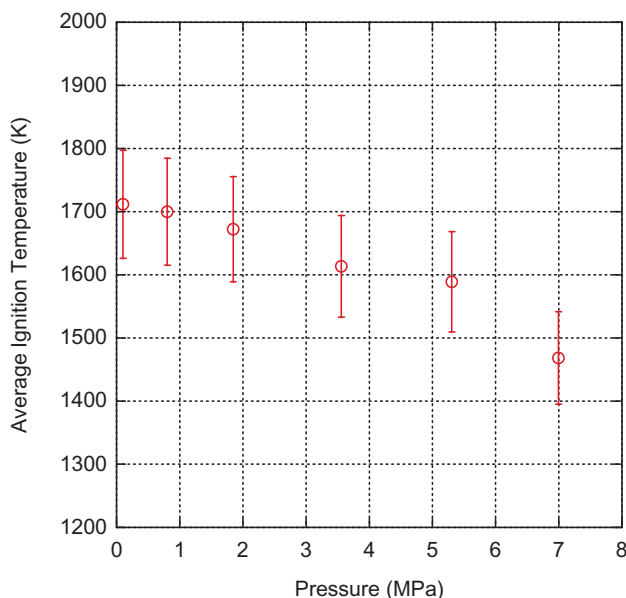
Figure 8 Average ignition temperatures of TiH$_2$ as a function of pressure (heating rate $\sim 1.3 \times 10^5$ K/s).

(1951) for titanium hydride. However, in our experiments the heating rate is significantly higher and a higher ignition temperature would be expected. No constant ignition temperature pressure regime was observed (Figure 8) unlike what we observed previously with aluminum hydride (Young et al., in press).

High Speed Imaging

High speed images (Phantom 7.3 high-speed camera) of ignition at low (1 atm) and high pressures ($\sim$3.6 MPa) are shown in Figures 9 and 10. The heating rate in both cases was set to approximately 1.3×10^5 K/s, and images were captured with a framing rate of 21,052 Hz. The reference time shown in the images, t_o, is the time at which the event being visualized was beginning.
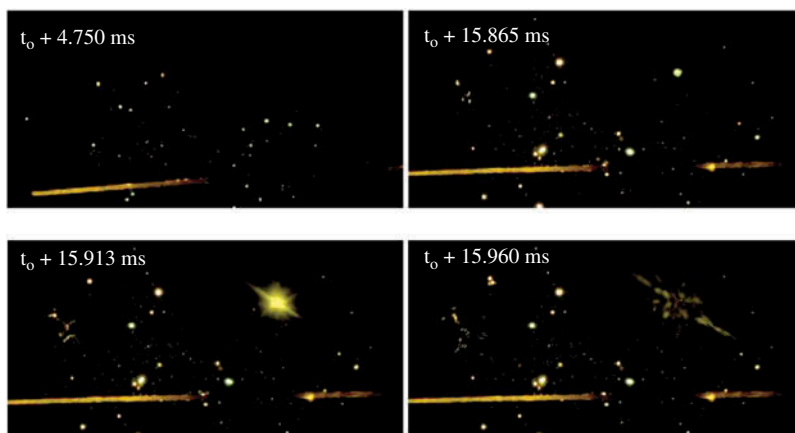

Figure 9 Titanium hydride ignition in air (1 atm with a heating rate of $\sim$1.3 $\times$ 10^5 K/s). The time series images clearly show the fragmentation of a particle.
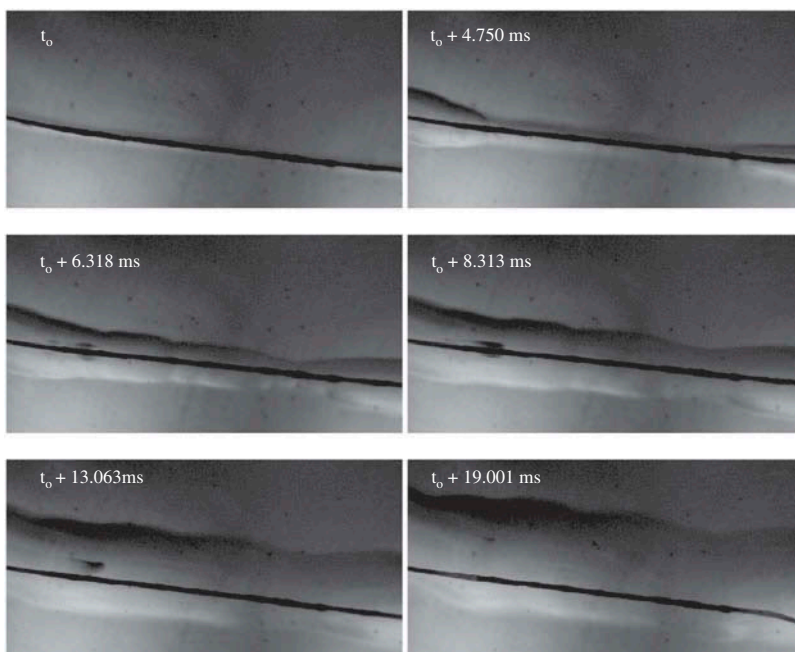

Figure 10 Titanium hydride ignition in air (3.6 MPa with a heating rate of $\sim$1.3 $\times$ 10^5 K/s).

Figure 9 is an example of the titanium hydride igniting in air at 0.101 MPa. Similar to aluminum hydride (Young et al., in press), particles that have achieved ignition can be seen leaving the heating filament in a fairly symmetric manner. Particle explosions were detected and an example can be seen in Figure 9, which contains three consecutive frames: before, during, and after a particle explosion. This behavior has been observed previously with pure titanium particles by other research groups (Badiola and Dreizin, 2013; Clark et al., 1975; Harrison, 1958; Molodetsky et al., 1998; Shafirovich et al., 2008), and was attributed to nitrogen from the ambient air dissolving into the particle during combustion.

Figure 10 is a series of shadowgraph images of titanium hydride ignition in air at 3.6 MPa. Density gradients can be clearly seen, and are not observed for bare wires, which we attribute to the reaction between hydrogen and air based upon our previous study on aluminum hydride (Young et al., in press). Interestingly, unlike aluminum hydride, at elevated pressures the particles do not readily leave the heating filament during the ignition event. With AlH_3, we concluded that the violence of reaction between H_2 and air was the primary reason that the particles were ejected from the wire filament. By mass, AlH_3 contains about 10% hydrogen compared to about 4% for TiH_2. Therefore, for a given mass (or mole) there is less hydrogen available for reaction. Furthermore, the ability of TiH_2 to oxidize or form oxyhydrides during the dehydrogenation process, may serve to slow down dehydrogenation, and thus further reducing H_2 availability for gas-phase combustion. At higher pressures we expect the concentration of oxygen would be higher near the particle surface, and thus increase the likelihood and degree of oxidation or oxyhydride formation as compared to the lower pressures. Thus, we argue that the combined effects of decreased hydrogen evolution enable particles to remain on the surface of the filament.

Quenched Particle Inspection

Particles were captured and quenched after an ignition event on a SEM stage at a distance of approximately 2.5 mm from the heating filament for further analysis. Figure 11 provides representative images of two different quenched particles during the same experiment. The image on the left is of a particle that is very smooth, spherical in nature, and contains come crater-like features. This suggests that the particle has completely melted prior to quenching, but it is still of similar size to the original unreacted particle ($\sim$3 μm). The image on the right is of a particle, which is about 1 μm and does not appear to have fully melted yet. Although these particles are at different stages of their individual

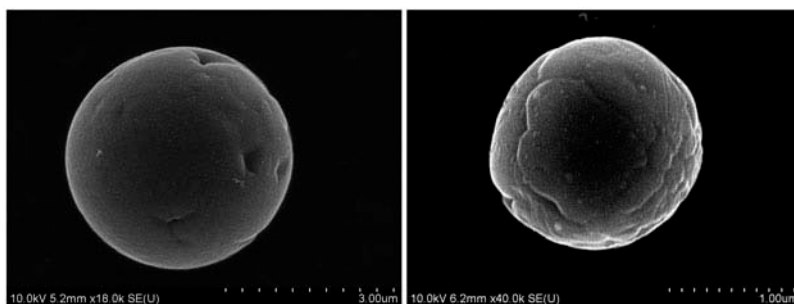**Figure 11** SEM images of quenched titanium hydride particles after combustion in air at 0.101 MPa.
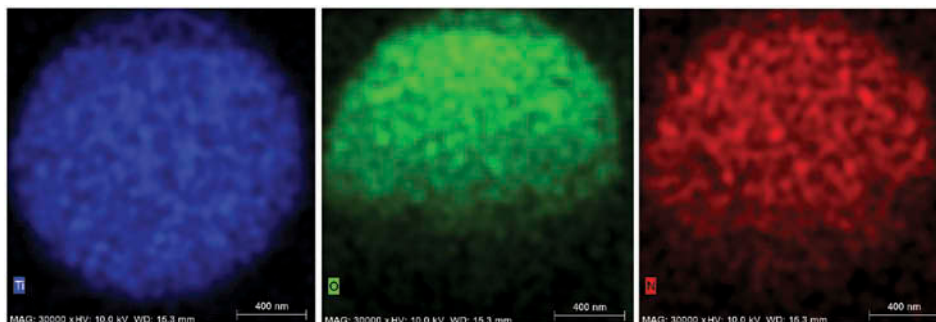
Figure 12 Elemental mapping of quenched titanium hydride particles by EDX.

combustion processes, they are both very clearly near their initial particle sizes. During titanium combustion, Shafirovich et al. (2008) observed that throughout the majority of the combustion process, the particle size remained approximately constant. Shafirovich et al. (2008) explained this result by comparing the densities and molecular masses of various oxides and nitrides of titanium and noting that they are similar. Following a similar analysis titanium hydride particles would be expected to grow in diameter by about 20% when forming TiO_2 compared to 17% for titanium conversion to TiO_2. Conversion to other oxides of titanium or even titanium nitride would result in less change in particle diameter.

Figure 12 is an elemental map obtained by energy dispersive X-ray spectroscopy (EDX) analysis of the particle on the left hand side of Figure 11. The main elements detected were titanium, nitrogen, and oxygen, all of which appear to be relatively uniformly distributed throughout the surface of the particle. Unfortunately, EDX cannot detect hydrogen, so we are unable to comment on any remnant hydrogen that might remain within the particle. Analyses of additional quenched particles produced similar results. This result is in agreement with previous observations of titanium combustion (Molodetsky et al., 1998), and would lead one to believe that the explosive behavior of the particles observed in this study is a result of nitrogen and oxygen dissolution into the titanium just as has been postulated for pure titanium, although it cannot be entirely ruled out that hydrogen bound in the particle contributed.

DISCUSSION

The dehydrogenation temperature at a heating rate of 1.3×10^5 K/s was about 900 K under vacuum conditions, while the ignition temperature at 1 atmosphere was about 1700 K, and dropped to about 1475 K at 7 MPa. Then, the resulting ignition delay from the onset of dehydrogenation is about 6 ms at 1 atmosphere compared to 4 ms at 7 MPa. This result suggests that pressure is not significantly adversely affecting the onset of the dehydrogenation process. In fact, pressure may have no effect on the onset of the dehydrogenation process at all.

During our earlier study on aluminum hydride (Young et al., in press), we found that the ignition temperature became independent of pressure above ∼0.4 MPa, which we concluded was a result of reaching explosion limits or at a minimum reaching autoignition limits of the H_2/air reaction. However, in this study, no constant ignition temperature regime was found in the range of pressures tested. Rather, ignition temperature decreased

over the entire pressure range approximately linearly. It seems likely then that this is due to significant differences in the local stoichiometry for the two materials caused by: (1) less available hydrogen in TiH_2 and (2) a reduction in dehydrogenation rates due to the formation of oxides or oxyhydrides during dehydrogenation. Since the explosion and ignitability limits of hydrogen are also dependent on stoichiometry, the reduction in local stoichiometry must have been sufficient to minimize these affects. However, hydrogen ignition is still impacted by the effects of pressure resulting in an overall observed decrease in ignition temperature. The PMT traces showed some erratic behavior at our highest pressure ($\sim$7 MPa), which was a characteristic of the H_2/air autoignition/explosive phenomenon with aluminum hydride (Young et al., in press) suggesting that if pressure were increased further a constant temperature ignition regime may be reached that would be governed by H_2/air autoignition or explosive limits.

CONCLUSIONS

In this study, we have evaluated the high heating rate decomposition, ignition, and combustion characteristics of titanium hydride by rapidly heating samples deposited on a filament. Decomposition studies were conducted for heating rates ranging from 8×10^4 K/s to 4×10^5 K/s. Under vacuum conditions the onset of dehydrogenation had an activation energy of about 47 kJ/mol and it appears to be a process that is limited by intraparticle diffusion of hydrogen.

Ignition studies in air at a heating rate of $\sim$$1.3 \times 10^5$ K/s for pressures ranging from atmospheric up to about 7 MPa, found the ignition temperature decreased approximately linearly as pressure increased, from 1700 K to 1475 K. Ignition delay from the onset of dehydrogenation decreased from about 6 ms to 4 ms as the pressure was increased from atmospheric to 7 MPa indicating that at a minimum the dehydrogenation process is not adversely impacted by increasing pressure.

During steady state combustion, titanium hydride displayed many similar characteristics to pure titanium particles including violent particle explosion. EDX inspection of post combustion quenched particles revealed that they consisted of titanium, oxygen, and nitrogen. This finding is also consistent with previous theories on titanium particle explosive phenomenon.

ACKNOWLEDGMENTS

REFERENCES

Ahluwalia, R.K., Hua, T.Q., and Peng, J.K. 2009. Automotive storage of hydrogen in alane. *Int. J. Hydrogen Energy*, **34**, 7731–7740.

Anderson, K., and Fleshman, W.S. 1950. Reactivity of titanium hydride with air. *Ind. Eng. Chem.*, **42**(7), 1381–1383.

Badiola, C., and Dreizin, E.L. 2013. Combustion of micron-sized particles of titanium and zirconium. *Proc. Combust. Inst.*, **34**(2), 2237–2243.

Borchers, C., Khomenko, T.I., Leonov, A.V., and Morozova, O.S. 2009. Interrupted thermal desorption of TiH_2. *Thermochim. Acta*, **493**(1–2), 80–84.

Clark, A.F., Moulder, J.C., and Runyan, C.C. 1975. Combustion of bulk titanium in oxygen. *Proc. Combust. Inst*., **15**(1), 489–499.

Connell, T.L., Risha, G.A., Yetter, R.A., Young, G., Sundaram, D.S., and Yang, V. 2011. Combustion of alane and aluminum with water for hydrogen and thermal energy generation. *Proc. Combust. Inst*., **33**(2), 1957–1965.

Fokin, V., Malov, Y., Fokina, S., Troitskaya, S., and Shilkin, S. 1995. Investigation of interactions in the TiH_2-O_2 system. *Int. J. Hydrogen Energy*, **20**(5), 387–389.

Gromov, A.R., Kouznetsov, N.N., Yuding, S.L., and Lunin, V.V. 1997. The investigation of titanium hydride oxidation process. *J. Alloys Compd*., **261**(1–2), 269–272.

Harrison, P.L. 1958. The combustion of titanium and zirconium. *Proc. Combust. Inst*., **7**(1), 913–918.

Hartman, I. 1951. The explosibility of titanium, zirconium, thorium, uranium, and their hydrides. USAEC Report No. 40-1562, Bureau of Mines.

Illekova, E., Harnuskova, J., Florek, R., Simancik, J., Matko, I., and Svec Sr., P. 2011. Peculiarities of TiH_2 decomposition. *J. Therm. Anal. Calorim*., **105**(2), 583–590.

Jian, G., Chowdhury, S., Sullivan, K., and Zachariah, M.R. 2013. Nanothermite reactions: Is gas phase oxygen generation from the oxygen carrier an essential prerequisite to ignition? *Combust. Flame*, **160**(2), 432–437.

Kennedy, A.R. 2002. The effect of TiH_2 heat treatment on gas release and foaming in Al-TiH_2 preforms. *Scr. Mater*., **47**, 763–767.

Kennedy, A.R., and Lopez, V.H. 2003. The decomposition behavior or as-received and oxidized TiH_2 foaming-agent powder. *Mater. Sci. Eng*., **A357**, 258–263.

Liu, H., He, P., Heng, J.C., and Cao, J. 2009. Kinetic study on nonisothermal dehydrogenation of TiH_2. *Int. J. Hydrogen Energy*, **34**, 3018–3025.

Matijasevic-Lux, B., Banhart, J., Fiechter, S., Gorke, O., and Waderka, N. 2006. Modification of titanium hydride for improved aluminum foam manufacture. *Acta Mater*., **54**, 1887–1900.

Molodetsky, I.E., Vicenzy, E.P., Dreizen, E.L., and Law, C.K. 1998. Phases of titanium combustion in air. *Combust. Flame*, **112**(4), 522–532.

Ozawa, T. 1965. A new method for analyzing thermogravimteric data. *Bull. Chem. Soc. Jpn*., **38**, 1881.

Ozawa, T. 1970. Kinetic analysis of derivative curves in thermal analysis. *J. Therm. Anal*., **2**, 301.

Rasooli, A., Boutorabi, M.A., and Divandari, M. 2013. The effect of high heating rate on the thermal decomposition behavior of titanium hydride (TiH_2) powder in air. *Bull. Mater. Sci*., **36**(2), 301–309.

Sakintuna, B., Lamari-Darkrim, F., and Hirscher, M. 2007. Metal hydride materials for solid hydrogen storeage: A review. *Int. J. Hydrogen Energy*, **32**, 1121–1140.

Samal, S., Cho, S., Park, D.W., and Kim, H. 2012. Thermal characterization of titanium hydride in thermal oxidation process. *Thermochem. Acta*, **542**, 46–51.

Shafirovich, E., Teoh, S.K., and Varma, A. 2008. Combustion of levitated titanium particles in air. *Combust. Flame*, **152**(1–2), 262–271.

Shark, S.C., Pourpoint, T.L., Son, S.F., and Heister, S.D. 2013. Performance of dicyclopentadiene-based hybrid rocket motors with metal hydride additives. *J. Propul. Power*, **29**(5), 1122–1129.

Stepura, G., Rosenband, V., and Gany, A. 2012. A model for the decomposition of titanium hydride and magnesium hydride. *J. Alloys Compd*., **513**, 159–164.

Young, G., Piekiel, N., Chowdhury, S., and Zachariah, M.R. 2010a. Ignition behavior of α-alane. *Combust. Sci. Technol*., **182**(7), 1341–1359.

Young, G., Risha, G.A., Miller, A.G., Glass, R.A., Connell, T.L., and Yetter, R.A. 2010b. Combustion of alane-based solid fuels. *Int. J. Energetic Mater. Chem. Propul*., **9**(3), 249–266.

Young, G., Jacob, R., and Zachariah, M.R. In press. High pressured ignition and combustion of aluminum hydride. *Combust. Sci. Technol*. DOI: 10.1080/00102202.2015.1038383.